

# Electromigration-based Deposition Enabled by Nanorobotic Manipulation Inside a Transmission Electron Microscope

Zheng Fan<sup>1</sup>, Xinyong Tao<sup>2</sup>, Xudong Cui<sup>3</sup>, Xudong Fan<sup>4</sup>, Xiaobin Zhang<sup>5</sup>, and Lixin Dong<sup>1,\*</sup>

<sup>1</sup>Department of Electrical and Computer Engineering, Michigan State University, East Lansing, MI 48824-1226, USA

<sup>2</sup>College of Chemical Engineering and Materials Science, Zhejiang University of Technology, Hangzhou 310014, China

<sup>3</sup>Department of Material Science & Technology, Research Center of Laser Fusion, China Academy of Engineering Physics, Mianyang, Sichuan 621900, China

<sup>4</sup>Center of Advance Microscopy, Michigan State University, East Lansing, MI 48824-1226, USA

<sup>5</sup>Department of Materials Science and Engineering, Zhejiang University, Hangzhou 310027, China

\*Email: ldong@egr.msu.edu

**Abstract**— *Electromigration-based deposition (EMBD) is an additive nanolithography technology for the fabrication of three-dimensional (3D) nanostructures. Key techniques for extending the capability of EMBD have been tackled experimentally including the deposition against a non-conductive surface, shape control of the as-deposited nanostructure, and continuous mass feeding. The process is based on nanofluidic mass delivery at the attogram scale from metal-filled carbon nanotubes (m@CNTs) using nanorobotic manipulation inside a transmission electron microscope. By attaching a conductive probe to the sidewall of the CNT, it has been shown that mass flow can be achieved regardless of the conductivity of the object surface. Experiments have shown the influence of heat sinks on the geometries of the deposits from EMBD. By modulating the relative position between the deposit and the heat sinks using dual probes, it has been possible to reshape the deposits. The limited mass encapsulated inside a CNT requires a frequent change of them for depositing large structures. To realize continuous feeding, a reservoir will be an excellent solution. We have observed that the copper inside the neighbor CNTs to the CNT injector can be sucked into the injector. Although the mechanism is not well understood yet, electromigration and atom-by-atom wall-passing-through may be responsible to this phenomenon. This observation enabled a new path for the design of an EMBD system. As a general-purposed nanofabrication process, EMBD will enable a variety of applications such as nanorobotic arc welding and assembly, nanoelectrodes direct writing, and nanoscale metallurgy.*

**Index Terms**—*electromigration, nanolithography, nanorobotic manipulation, nanofabrication, nanoassembly*

## I. INTRODUCTION

Additive nanolithography technologies such as electron-beam-induced deposition (EBID) [1-6] and focused ion-beam chemical vapor deposition (FIB-CVD) [7-9] are of growing interest for the fabrication and interconnection of three-dimensional (3D) nanostructures such as atomic force microscope (AFM) cantilever tips [10, 11], helical nanostructures [7], gripper fingers, and other nanostructures [12]. Electromigration-based deposition (EMBD) is an emerging technique in this category, with which the deposition of materials to a surface is caused by the movement of the ions on the opposite direction of current in a conductor due to the momentum transfer between

conducting electrons and diffusing metal atoms. Previous development has shown some unique applications such as attogram-scale mass transport [13, 14], nanorobotic spot welding [15], nanofluidic junctions [16], and spherical nanostructure formation [17]. However, several key technologies are remaining to be tackled. Firstly, all of the above-mentioned technologies require that the objective surface to be conductive. Deposition against a non-metallic object surface is not available because an electric circuit is needed for the electromigration (Fig. 1(a)). Secondly, the post modification of the geometries of deposits is limited by the thermal energy distribution in the loop, because the probes typically have a larger thermal capacitance than the nanochannels and the deposits, which made it impossible to reheat and reshape the as-deposited nanostructures. Against an object surface with excellent thermal conductivity, e.g., an Au-coated tungsten probe used in the experiment, the shapes and sizes are determined instantly by the materials flowing out from a carbon nanotube (CNT). Reheating or reshaping is unattainable because the minimum thermal energy exists at the deposition site between the nanotube tip

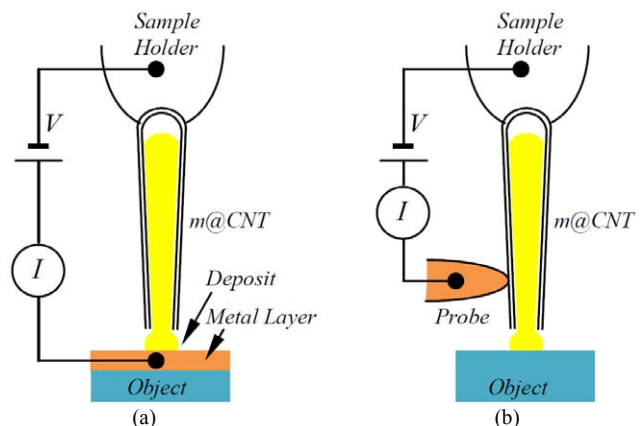


Fig. 1 Schematic of electromigration-based deposition (EMBD). The metal filled CNT (m@CNT) is used as an injector for deposition. By applying a bias, the encapsulated metal can be flowed out for deposition. (a) A metal layer on the object surface is necessary to form the electric circuit for EMBD. (b) By using a probe attaching to the sidewall of the m@CNT, the surface of the object can be either conductive or insulate.

and the probe (heat sink). Hence, the feeding rate of the copper from the nanotube and the positioning of the nanotube tip are the main factors to be considered in determining the geometries of the deposition. On the other

hand, if the object surface is thermal and electric resistive, e.g., another nanotube as used in the experiment, reheating and reshaping will be possible, which provides a post-process method for such applications as the fabrication of spherical nanostructures, removing welded nanostructures, and free-shape prototyping. Finally, the source of materials to be deposited is limited by the volume of the nanotubes. Continuous feeding is impossible. Here we report an observation that the copper inside the neighbor CNTs to the CNT injector can be sucked into the injector, which will enable a new path to continuous feeding for EMBD systems.

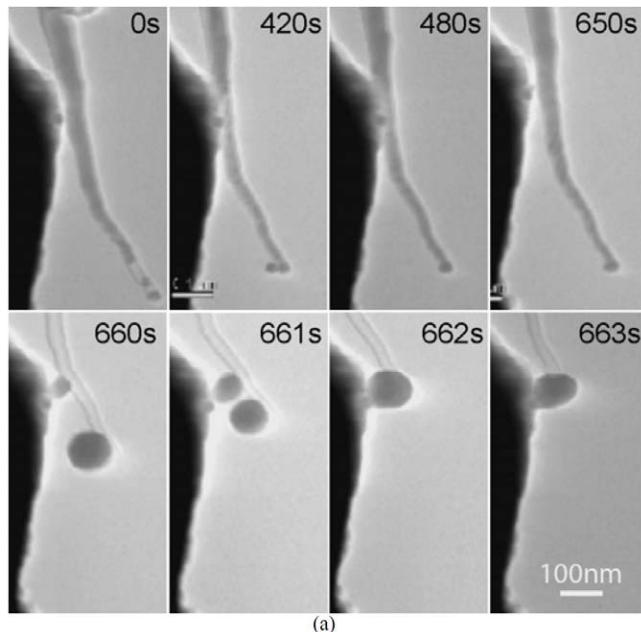
## II. TOWARDS THE DEPOSITION TO NON-CONDUCTIVE SURFACE

To apply EMBD against a non-conductive surface, an electrical circuit must be formed without involving the surface. This can be implemented by taking the architecture as shown in Fig. 1 (b). The difference in architecture from the conventional one (Fig. 1(a)) is that the electromigration will only occur between the probe and the sample holder rather than in the entire tube. The thermal energy generated in this part can be transported to the tip part between the probe and the nanotube tip so that the encapsulated materials in the tip part will be passively pushed out by the rare segment between the probe and the sample holder.

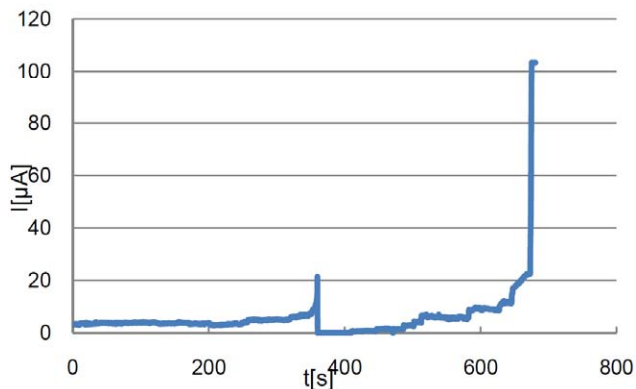
Our experiments were performed in a transmission electron microscope (TEM, JEOL 2200FS) with a field emission gun. The samples we used were Cu-filled CNTs, which are synthesized using an alkali-doped Cu catalyst by a thermal CVD method [18], and their outer diameters are in a range of 40-80 nm. The single crystalline Cu nanoneedles are encapsulated in graphite walls, approximately 4 to 6 nm thick, at the tips of CNTs.

A scanning tunneling microscope built in a TEM holder, FM2000E STM-TEM holder (Nanofactory Instruments AB), is adopted for the experiments. The probe can be positioned in a millimeter-scale workspace with sub-nanometer resolution with the STM unit actuated by a three-degree-of-freedom piezotube, making it possible to select a specific CNT. Physical contact can be made between the probe and the sidewall of a nanotube. Applying a voltage between the probe and the sample holder establishes an electrical circuit through a CNT and injects thermal energy into the system via Joule heating. By increasing the applied voltage, the local temperature can be increased past the melting point of the copper encapsulated in a tube. Then, the encapsulated materials may deliver from the carbon shells and deposit on a surface.

Experimental results are shown in Fig. 2. Fig. 2 (a) are TEM images (video frames) showing the EMBD using the configuration shown in Fig. 1(b). The dark area is the probe tip of the manipulator. The initial mass inside the CNT is estimated to be 5.7 fg at 0 s based on the high resolution TEM images and the density of copper ( $8.92 \text{ g}\cdot\text{cm}^{-3}$ ). At 663 s, 4.4 fg (77.2%) has deposited while the rest mass evaporated and/or diffused onto the surface of the probe. It can be seen that at 0 s, there was an empty section close to



(a)



(b)

Fig. 2 (a) TEM images recorded the EMBD using the configuration shown in Fig. 1(b). The initial mass inside the CNT is estimated to be 5.7 fg at 0 s. At 663 s, 4.4 fg (77.2%) has deposited while the rest mass evaporated and/or diffused onto the surface of the probe. It can be seen that at 0 s, there was an empty section close to the tip of the CNT, which was filled up at 420 s; showing that the flow started inside the CNT. The extra sphere at the CNT tip was a result of that. The fact that the transport direction was pointing to the CNT tip confirmed that the electromigration is responsible for this flow. Then, at 480 s, the volume of the sphere at the CNT tip decreased as a result of evaporation. There was no obvious change occurred till the moment at 650 s. At 660 s, within 3 seconds, the CNT was drained off and a large sphere formed on the CNT tip. Because the distance between the deposit and the probe is small and the contact between the probe and the CNT was not firm, the CNT slid back and the deposit dropped onto the probe. (b) The current-time curve recorded during the whole process. The peak at 360 s represent that the contact resistance between the probe and the CNT improved, which was caused by relative slipping of the probe and the CNT. Before and after that moment, no obvious changes of the current have been observed. During the same period, no remarkable mass flow has occurred according to the video. When the flow started at 660 s, an abrupt inflation of the current has been monitored, in the meantime, the CNT was drained off and a large spherical deposit (diameter: 37.5 nm) appeared at the CNT tip.

the tip of the CNT, which was filled up at 420 s; showing that the flow started inside the CNT. The extra sphere at the CNT tip was a result of that. The fact that the transport direction was pointing to the CNT tip confirmed that the electromigration was responsible for this flow. Then, at 480 s, the volume of the sphere at the CNT tip decreased as a result of evaporation. There was no obvious change occurred till the moment at 650 s. At 660 s, within 3 seconds, the CNT was drained off and a large sphere formed on the CNT tip. Because the distance between the deposit and the probe is small and the contact between the probe and the CNT was not firm, the CNT slid back and the deposit dropped onto the probe. Figure 2 (b) is the current-time curve recorded during the whole process. The peak at 360 s represents that the contact resistance between the probe and the CNT improved, which was caused by relative slipping of the probe and the CNT. Before and after that moment, no obvious changes of the current have been observed. During the same period, no remarkable mass flow has occurred according to the video frames (Fig. 2(a)). When the flow started at 660 s, an abrupt inflation of the current has been monitored, in the meantime, the CNT was drained off and a large spherical deposit (diameter: 37.5 nm) appeared at the CNT tip.

### III. SHAPING THE DEPOSITS

In this investigation, in order to reveal the factors that

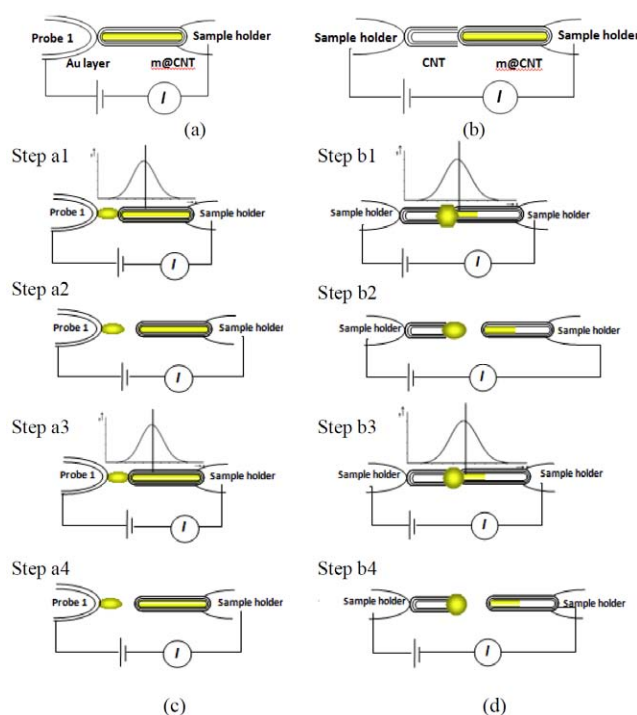


Fig. 3 Schematic setup and the process of EMBD (a) The experiment setup for the EMBD on the surface with excellent electric and thermal conductivity. (b) The experiment setup for the EMBD on the surface with resistive conductivity. (c) The processes for the EMBD against a conductive surface (an Au-coated W-tip). (d) The processes for the EMBD against a resistive surface (an empty CNT).

determine the geometries of deposits from EMBD, experiments were performed with two setups: (1) the Cu-filled CNT is positioned against an excellent conductor and (2) the Cu-filled CNT is positioned against a resistive surface. Here we use a tungsten probe (length: 10  $\mu\text{m}$ , tip radius: 100nm) coated by a gold thin film (21nm thick) for (1), and an empty CNT for (2). The setups for (1) and (2) are shown schematically in Fig. 3(a) and (b), and the processes are shown in Fig. 3(c) and (d). Qualitative distribution of the thermal energy has been attached to some panels in Fig. 3(c) and (d). As illustrated in Fig. 3(a) and (c), when the Cu-filled CNT contacts to the probe, due to the larger thermal energy capacitance of the probe than the CNT, the heat sinks locate at the interface between the CNT and the probe, where the temperature is the lowest. Reattaching the Cu-filled CNT to the deposit once the deposition is finished, the shape of the deposit will not be able to be changed. In the second case, by

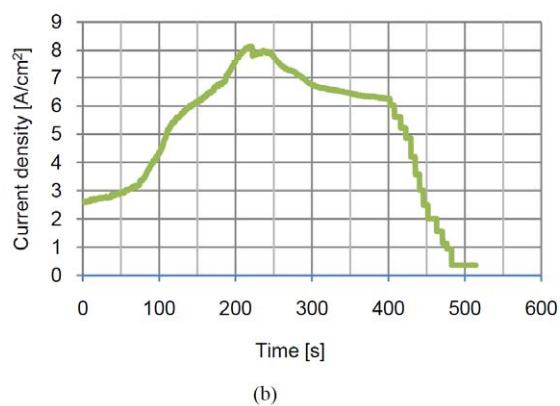
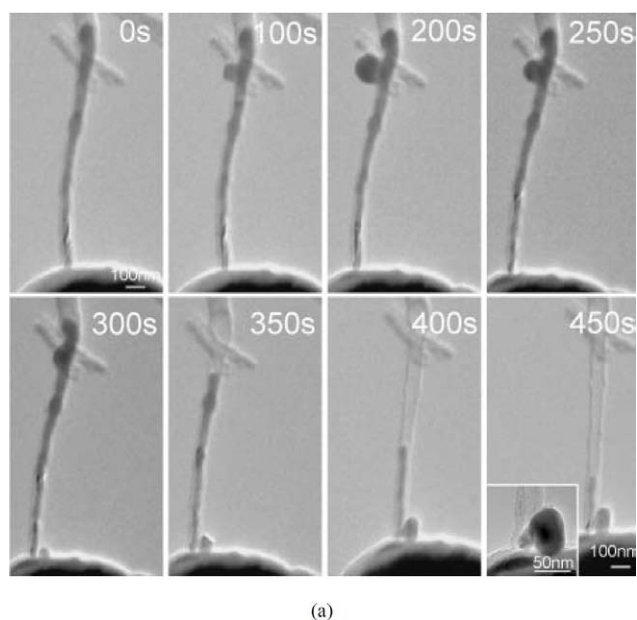


Fig. 4 (a) TEM images (video frames) of EMBD against a thermal conductive surface. (b) Current density vs. time curve of the EMBD process.

replacing the probe with an empty CNT, the deposit location will have a higher temperature when the Cu-filled CNT reattaches to the empty CNT. Then, the deposit will be reheated and the shape can be changed.

### A. Instant shaping

This experiment is designed to justify that it is impossible to reshape the deposit from EMBD in the case of Fig. 3 (a). Selected video frames of the EMBD processes in an experiment are shown in Fig. 4(a). By increasing the bias from 0 V at a step of 0.1 V, the inner copper core flowed out to the tip of CNT when it reached 2.0V.

The current density vs. time curves were obtained during the process (Fig. 4(b)). An obvious current density drop from the peak at about  $8.1 \times 10^6 \text{ A/cm}^2$  occurred at 210 s as the flowing began, which we attribute to resistance increase of the tube due to the exposure of the carbon shells along with the draining of the encapsulated copper, which has better conductivity than carbon [15]. On the continuous deposition of metal on the probe, the deposit shape was formed instantly due to the excellent thermal conductivity of the probe that

cools down the deposit in a short time. Reheating of the cooled-down deposit was unable to be achieved because the volume of the probe (tip radius: 120 nm, root radius:  $10 \mu\text{m}$ ) is absolutely larger than that of the copper deposit. The probe serves as a heat sink with essentially infinite capacity compared with the copper deposit. As a result, the experiment of EMBD on the surface with excellent thermal conductivity showed that although the deposition of copper from the nanotube occurred in a short time, the cooling down of deposit was also instant due to the heat sink of probe, therefore, the reheating or reshaping was unattainable due to the minimum distribution of thermal energy at the deposition site between the nanotube tip and the probe (heat sink).

### B. Shape Control of Deposits

The same EMBD procedure has been applied to the single CNT. Figure 5(a) to (c) show the process of mass delivering to the interconnection of the tips and the shape control of the deposit. The process was recorded by real-time video, and the main procedures can be divided into two parts, the

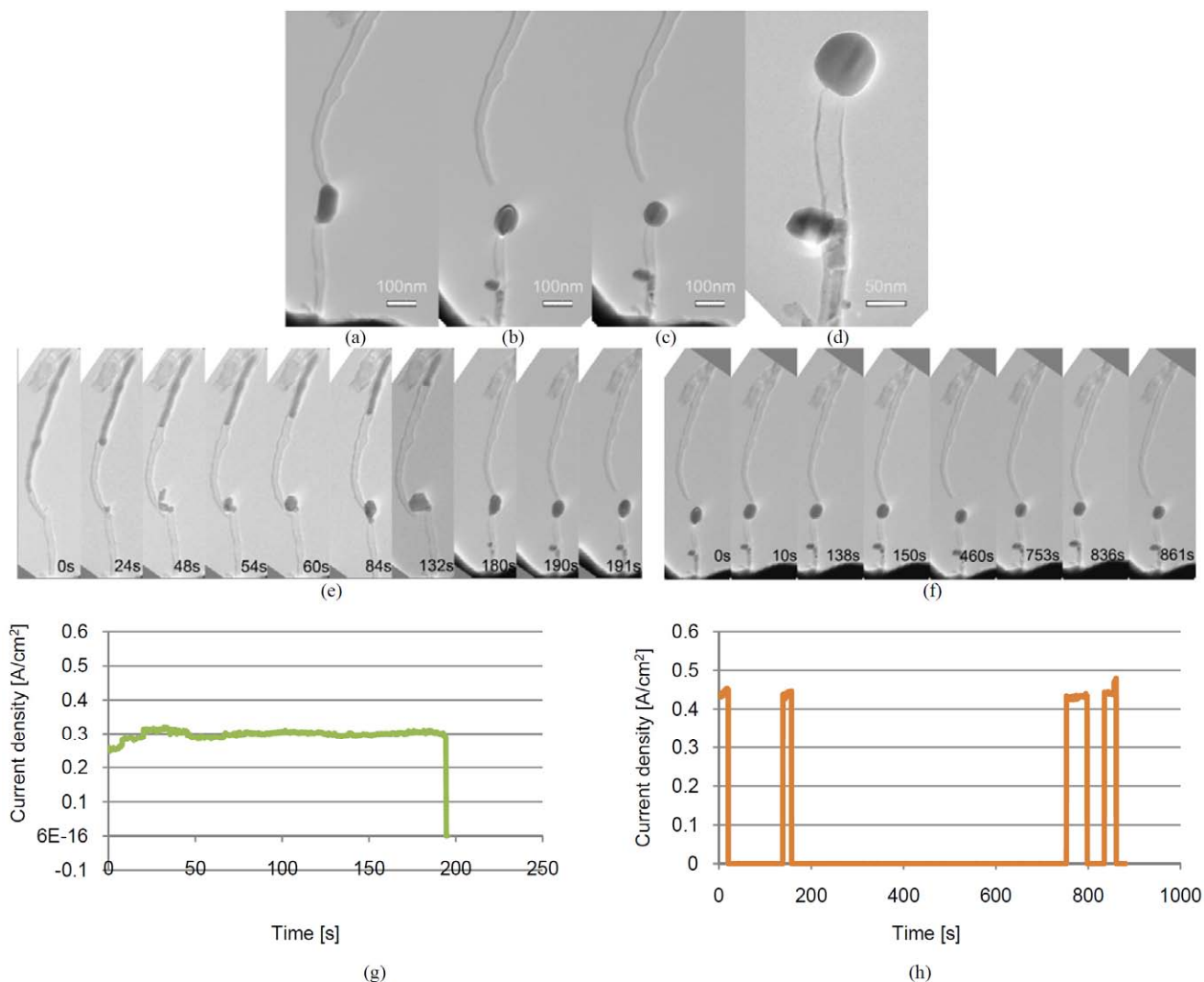


Fig. 5 EMBD processes on a thermally/electrically resistive object. (a) Metal flows out from a copper-filled CNT. (b) A spherical deposit on the tip of a CNT by EMBD. (c) EMBD shape control process. (d) Modified nanostructure on the tip. (e) EMBD process recorded by video. (f) Shape control process recorded by video. (g, h) Current density vs. time curves for EMBD and shape control.

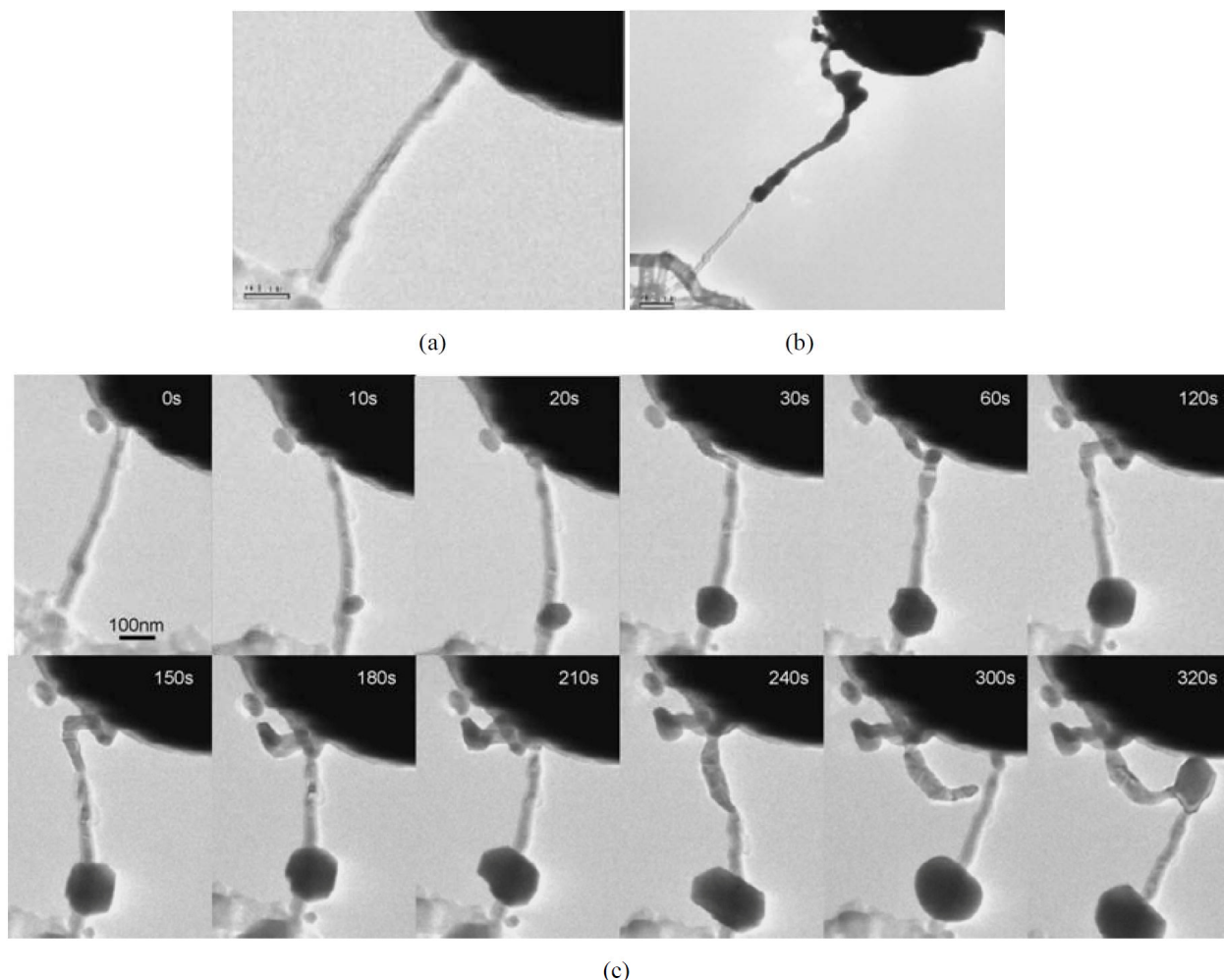


Fig. 6 Continuous feeding of Cu from neighbor CNTs. The initial mass inside the nanotube injector is 1.9 fg (a), while the deposited mass shown in (b) is 29.0 fg (about 15 times more than the original mass). (Scale bars: (a) 100 nm, (b) 200 nm). (c) Nanostructures “written” by EMBD with continuous feeding.

EMBD process on CNT (Fig. 5(e)) and the shape control of deposit (Fig. 5(f)). In this experiment, the EMBD started at 2.05 V, and the entire process had continued for about 191 s. The mass flow rate was found to be 3.27 nm/s according to the length change of the inner copper core. The flowing out of copper reveals that a copper polyhedral nanoparticle initially formed on the tip of the tube. As shown in the first panel of Fig. 3(d), the middle point of the nanotube is the hottest spot. So, we positioned the polyhedral deposit close to the length center of two CNTs, which is close to the hottest position of the interconnected system. Therefore, the deposited metal will remain in the molten status and the shape of polyhedral could be changed by pulling in and out of the deposit.

The shape control of deposit is shown in Fig. 5(f). The sphere formed from the above processes cooled down when the two tips depart from each other and then reheated by reconnecting the two nanotubes. As a result, reshaping of the deposit is achieved by contacting the tube to the deposit at a certain position. Figure 5(d) shows the reshaped nanostructure. From the current density vs. time curves depicted in Fig. 5 (g) and (h), we can see that the thermal

energy to reshape the deposit is lower during the deposit process, and the current density kept in a steady value ranging from  $0.25 \times 10^6$  to  $0.35 \times 10^6$  A/cm<sup>2</sup> until the departure of the two tubes. During the reshaping of the deposits, the current density was about  $0.45 \times 10^6$  A/cm<sup>2</sup> when the two nanotubes contacted, which is higher than that for the EMBD process due to the higher resistivity of the drained-off nanotubes. The cooled-down nanostructures would be reheated and melted under a higher current density.

#### IV. CONTINUOUS FEEDING

The limited mass encapsulated inside a CNT requires a frequent change of them for depositing large structures. To realize continuous feeding, a reservoir will be an excellent solution. We have observed that the copper inside the neighbor CNTs to the CNT injector can be sucked into the injector (Fig. 6). The initial mass inside the nanotube injector is 1.9 fg (Fig. 6(a)), while the deposited mass shown in Fig. 6(b) is 29.0 fg. It is obvious that the extra mass (the mass in the deposit is about 15 times more than the original mass) is from the sources outside of the CNT. Although the

mechanism is not very well understood yet, electromigration-induced inter-tube mass transport is most likely responsible to this phenomenon. This involves the motion of the copper atoms passing through the CNT walls atom-by-atom. Continuous feeding has been used to “write” large nanostructures (Fig. 6(c)) by manually positioning the injector. This is of particular interest for such applications as arc welding and assembly, nanoelectrodes direct writing, and nanoscale metallurgy, where relatively large amount of mass are needed in the process.

## V. CONCLUSIONS

In summary, we have experimentally investigated several key techniques for extending the capability of EMBD including the deposition against a resistive surface, shape control of the as-deposited nanostructure, and continuous mass feeding. By attaching a conductive probe to the sidewall of the CNT, it has been shown that mass flow can be achieved regardless of the conductivity of the object surface. Experiments have shown the influence of heat sinks on the geometries of the deposits from EMBD. By modulating the relative position between the deposit and the heat sinks using two CNTs, it has been possible to reshape the deposits. We have observed that the copper inside the neighbor CNTs to the CNT injector can be sucked into the injector, which promises that continuous feeding is feasible. Although the mechanism is not well understood yet, electromigration and atom-by-atom wall-passing-through may be responsible to this phenomenon. As a general-purpose nanofabrication process, EMBD will enable a variety of applications such as nanorobotic arc welding and assembly, nanoelectrodes direct writing, and nanoscale metallurgy.

## REFERENCE

- [1] H. W. P. Koops, J. Kretz, M. Rudolph, and M. Weber, "Constructive 3-Dimensional Lithography with Electron-Beam-Induced Deposition for Quantum Effect Devices," *Journal of Vacuum Science & Technology B*, vol. 11, pp. 2386-2389, Nov-Dec 1993.
- [2] H. W. P. Koops, J. Kretz, M. Rudolph, M. Weber, G. Dahm, and K. L. Lee, "Characterization and Application of Materials Grown by Electron-Beam-Induced Deposition," *Japanese Journal of Applied Physics Part 1-Regular Papers Short Notes & Review Papers*, vol. 33, pp. 7099-7107, Dec 1994.
- [3] S. Matsui, "Nanostructure fabrication using electron beam and its application to nanometer devices," *Proceedings of the IEEE*, vol. 85, pp. 629-643, Apr 1997.
- [4] L. X. Dong, F. Arai, and T. Fukuda, "Electron-beam-induced deposition with carbon nanotube emitters," *Applied Physics Letters*, vol. 81, pp. 1919-1921, Sept. 2002.
- [5] W. Ding, D. A. Dikin, X. Chen, R. D. Piner, R. S. Ruoff, E. Zussman, X. Wang, and X. Li, "Mechanics of hydrogenated amorphous carbon deposits from electron-beam-induced deposition of a paraffin precursor," *Journal of Applied Physics*, vol. 98, art. no. 014905, Jul 2005.
- [6] G. Q. Xie, M. H. Song, K. Furuya, D. V. Louzguine, and A. Inoue, "Compound nanostructures formed by metal nanoparticles dispersed on nanodendrites grown on insulator substrates," *Applied Physics Letters*, vol. 88, p. 263120, Jun 2006.
- [7] S. Matsui, T. Kaito, J. Fujita, M. Komuro, K. Kanda, and Y. Haruyama, "Three-dimensional nanostructure fabrication by focused-ion-beam chemical vapor deposition," *Journal of Vacuum Science & Technology B*, vol. 18, pp. 3181-3184, Nov-Dec 2000.
- [8] M. Nagase, H. Takahashi, Y. Shirakawabe, and H. Namatsu, "Nano-four-point probes on microcantilever system fabricated by focused ion beam," *Japanese Journal of Applied Physics Part 1-Regular Papers Short Notes & Review Papers*, vol. 42, pp. 4856-4860, Jul 2003.
- [9] R. Kometani, K. Kanda, Y. Haruyama, T. Kaito, and S. Matsui, "Evaluation of field electron emitter fabricated using focused-ion-beam chemical vapor deposition," *Japanese Journal of Applied Physics Part 2-Letters & Express Letters*, vol. 45, pp. L711-L713, Jul 2006.
- [10] K. L. Lee, D. W. Abraham, F. Secord, and L. Landstein, "Submicron Si Trench Profiling with an Electron-Beam Fabricated Atomic Force Microscope Tip," *Journal of Vacuum Science & Technology B*, vol. 9, pp. 3562-3568, Nov-Dec 1991.
- [11] D. J. Keller and C. C. Chou, "Imaging Steep, High Structures by Scanning Force Microscopy with Electron-Beam Deposited Tips," *Surface Science*, vol. 268, pp. 333-339, May 1992.
- [12] L. X. Dong, F. Arai, and T. Fukuda, "Destructive Constructions of Nanostructures with Carbon Nanotubes through Nanorobotic Manipulation," *IEEE/ASME Transactions on Mechatronics*, vol. 9, pp. 350-357, June 2004.
- [13] K. Svensson, H. Olin, and E. Olsson, "Nanopipettes for metal transport," *Physical Review Letters*, vol. 93, art. no. 145901, Oct 2004.
- [14] P. M. F. J. Costa, D. Golberg, M. Mitome, S. Hampel, A. Leonhardt, B. Buchner, and Y. Bando, "Stepwise current-driven release of attogram quantities of copper iodide encapsulated in carbon nanotubes," *Nano Letters*, vol. 8, pp. 3120-3125, Oct 2008.
- [15] L. X. Dong, X. Y. Tao, L. Zhang, X. B. Zhang, and B. J. Nelson, "Nanorobotic spot welding: Controlled metal deposition with attogram precision from copper-filled carbon nanotubes," *Nano Letters*, vol. 7, pp. 58-63, Jan. 2007.
- [16] L. X. Dong, X. Y. Tao, M. Hamdi, L. Zhang, X. B. Zhang, A. Ferreira, and B. J. Nelson, "Nanotube fluidic junctions: Internanotube attogram mass transport through walls," *Nano Letters*, vol. 9, pp. 210-214, Jan 2009.
- [17] Z. Fan, X. Y. Tao, X. D. Cui, X. D. Fan, and L. X. Dong, "Spheres on Pillars: Nanobubbling Based on Attogram Mass Delivery from Metal-Filled Nanotubes," in *Proc. of the 10th IEEEConf. on Nanotechnology (IEEE-NANO2010)*, Seoul, Korea, 2010.
- [18] X. Y. Tao, X. B. Zhang, J. P. Cheng, Z. Q. Luo, S. M. Zhou, and F. Liu, "Thermal CVD synthesis of carbon nanotubes filled with single-crystalline Cu nanoneedles at tips," *Diamond and Related Materials*, vol. 15, pp. 1271-1275, Sep 2006.